Ultrafast nonequilibrium stress generation in gold and silver

O. B. Wright*
Electronics Research Laboratories, Nippon Steel Corporation, 5-10-1 Fuchinobe, Sagamihara, Kanagawa, 229 Japan
(Received 15 December 1993)

The dynamics of coherent phonon generation by femtosecond optical pulses in thin gold and silver films is studied using a pump and probe scheme. Detection is achieved by monitoring ultrafast surface vibrations in real time using laser-beam deflection. The phonon strain pulse shapes can be explained through the nonequilibrium coupling of the electron and phonon distributions, suggesting a new method for measuring the electron-phonon coupling constant.

The transient difference in the electron and lattice temperatures in metals after excitation with ultrashort laser pulses has been the topic of much recent research. The small specific heat of the electron gas allows electron temperatures of thousands of degrees to be generated for times up to a few picoseconds. This nonequilibrium imbalance in the electron and phonon distributions has been probed in several ways.[1-7] Although the initial experimental evidence came from studies of the laser-induced emission of photons or electrons from metal surfaces,[1] femtosecond thermomodulation techniques sensitive to hot electron relaxation and heat transport have played a particularly important role.[2-6] Thin films excited by ultrashort pump optical pulses are interrogated by recording the intensity modulation of delayed probe pulses. Taking into account the different response to changes in the electron and lattice temperatures, electron-phonon (e-p) coupling constants of a wide variety of metals were derived, constants which are also crucial to areas as diverse as superconductivity[8] and laser-induced melting.[9] More recently, photoelectric emission experiments continue to reveal more details of these nonequilibrium processes: the thermalization of photoexcited electron-energy distributions in metals through electron-electron coupling can be directly measured from the energy spectrum of photoelectrons associated with a delayed probe pulse.[7]

The nonequilibrium dynamics of the space- and time-dependent electron and phonon distributions also governs the generation of acoustic-phonon pulses in metals by ultrashort laser pulses.[10,11] The laser photons, absorbed near the surface of the metal, excite electrons with energies up to the region of the Fermi level to higher available states. The propagation, diffusion, and relaxation of the hot electrons determine the final profile of the phonon strain propagating away from the metal surface and result in a broadening of this phonon pulse. Initial results supporting this reasoning were recently obtained for group-VI transition metals using picosecond laser pulses and a beam deflection technique for direct phonon strain pulse detection from ultrafast surface vibrations.[12] Unlike piezoreflectance detection,[10] difficulties in relating the dynamic changes in optical reflectivity to the phonon strain are avoided.

In this paper, I report on the ultrafast stress generation in noble metals using polycrystalline films of gold and silver with femtosecond optical excitation and beam deflection detection. These metals were chosen because the e-p coupling is relatively weak, thus making e-p pulse broadening effects particularly pronounced and minimizing any spurious pulse distortion effects caused by acoustic attenuation. In addition, abundant comparative data are available on nonequilibrium electron-energy distributions in these materials, which approximate to free-electron metals near the Fermi energy. Gold and silver thus provide us the first reliable test cases for theories of ultrafast laser generation of acoustic phonons in metals.

Pump pulses of energy 2 eV (630-nm wavelength), of duration 200 fs [full width at half maximum (FWHM)], and repetition rate 76 MHz from a mode-locked dye laser are used to excite the phonons. Focusing to a spot diameter of about 20 μm allows incident pump fluences up to 0.6 mJ cm^{-2} to be obtained. The cross-polarized, weaker ($\sim$5% of pump) probe pulses are focused to a similar spot size to partially overlap with the pump spot. Changes in surface profile associated with phonon pulses returning to the surface lead to an angular deflection ($\delta\theta \sim 1$ μrad) of the probe beam, proportional to the surface displacement ($\delta z \sim 0.001$ nm), which is monitored with a dual-cell photodiode. Full details of the apparatus are given elsewhere.[12] The films are made by rf magnetron sputtering (at 60 and 100 nm/min for Au and Ag) on silica substrates. Examination of the film surfaces with an electron microscope revealed a wide distribution of grain sizes with an average diameter of $\sim$100 nm. Film thicknesses were calculated from the known sound velocities of the polycrystalline materials [$v = 3360$ and 3790 ms^{-1} for Au and Ag, respectively (Ref. 13)] and verified by needle profiling.

Figures 1 and 2 show the results for $\delta\theta$ as a function of delay time for Au and Ag films of thickness 470 and 245 nm, respectively. Echoes arise from longitudinal acoustic-phonon pulses bouncing backwards and forwards inside the film. Owing to the difference in reflectance at 2 eV, the signal-to-noise ratio for Au is better than for Ag. The approach commonly used to interpret the phonon pulse shapes is a one-dimensional thermoelastic model in the acoustic near field.[10-12] Energy absorbed in the region of the optical skin depth ($\zeta \approx 15$ nm for Au and 12 nm for Ag) results in a thermal expansion that launches a longitudinal strain pulse into the metal,

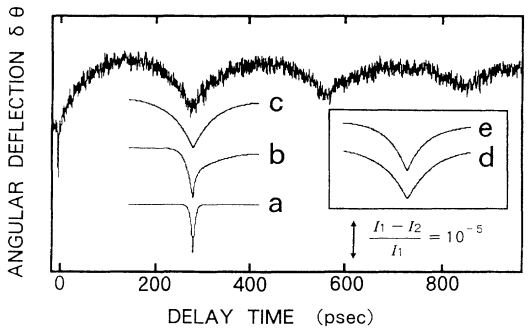

FIG. 1. Angular deflection of the probe laser beam against pump-probe delay time for a 470-nm film of Au at a pump fluence of 0.6 mJ cm^{-2}. Fit to first echo from the thermoelastic model (curve *a*), fit from the thermoelastic model including thermal diffusion (curve *b*), and fit from the nonequilibrium model with electron-phonon coupling parameter $g=16\times10^{15}$ W m^{-3} K^{-1} (curve *c*). (I_1 and I_2 refer to the intensities at the dual-cell photodetector.) The inset shows curves from the nonequilibrium model for $g=10\times10^{15}$ W m^{-3} K^{-1} (curve *d*) and $g=22\times10^{15}$ W m^{-3} K^{-1} (curve *e*).

$$\eta_{33}(z,t)=-\eta_0\mathrm{sgn}(z-vt)\exp[\,|z-vt|/\zeta\,]\ ,$$

for times $\gg\zeta/v$, as shown in Fig. 3(a). Integrating with respect to depth z gives the normal surface displacement, $u_{33}(t)=2\eta_0\zeta\exp(-v|t|/\zeta)$ (where $t=0$ corresponds here to the echo arrival), as shown by curves *a* of Figs. 1 and 2. The predicted pulse durations ($\sim$10 ps) are approximately twice the acoustic transit time ($2\zeta/v$) across the skin depth. Clearly, this model totally fails to account for the remarkably broadened widths of order 100 ps. (The slight smoothing effect of the laser pulse duration is included in all the fits.)

Several mechanisms for pulse distortion exist. Angular deflection caused by strain-induced radial gradients in the dielectric constants is estimated to be negligible at the present probe wavelength.[14] Temperature-induced radial gradients and the relaxing thermal expansion lead to the slowly varying background variation.[12] However, this too does not appreciably affect the observed pulse shapes. Broadening due to frequency-dependent attenuation can be estimated from available data for gigahertz acoustic

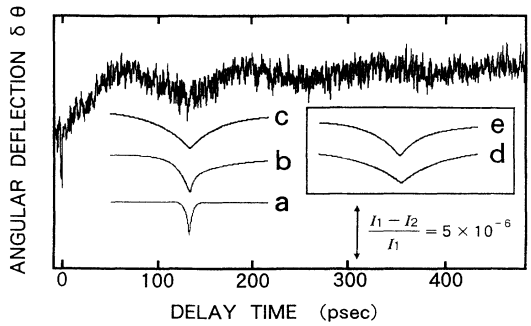

FIG. 2. Angular deflection of the probe laser beam against pump-probe delay time for a 245-nm film of Ag at a pump fluence of 0.6 mJ cm^{-2}. The fits (curves *a*–*e*) are as in Fig. 1, with $g=35\times10^{15}$ W m^{-3} K^{-1} (curve *c*), $g=15\times10^{15}$ W m^{-3} K^{-1} (curve *d*), and $g=55\times10^{15}$ W m^{-3} K^{-1} (curve *e*).

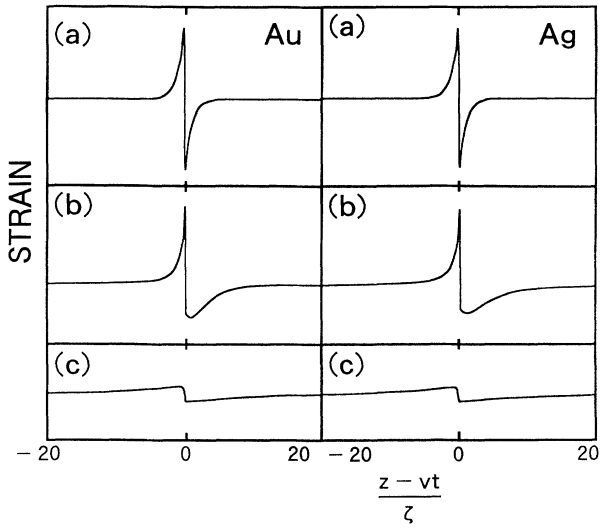

FIG. 3. Strain pulse shapes for Au and Ag, plotted as a function of the dimensionless parameter $(z-vt)/\zeta$, calculated according to (a) the thermoelastic model, (b) the thermoelastic model including thermal diffusion, and (c) the nonequilibrium model for a pump fluence of 0.6 mJ cm^{-2}. The scales for (a)–(c) are the same.

losses in Ag films, losses mainly caused by grain boundary scattering ($\propto\omega^2$, ω the angular frequency).[15] The calculated pulse distortion is not significant for phonon propagation distances ~1 μm (taking into account a scaling factor to correct for the different grain size).[16] Similar reasoning can be applied to Au. Dispersion is also negligible in the gigahertz range.

The thermoelastic model can be refined to account for the effect of heat flow.[10] The temperature distribution $T(z,t)$ in the film is calculated from Fourier's law in one dimension, assuming that the electrons and phonons in the metal remain in thermal equilibrium. This changing temperature distribution creates a stress pulse, which can be calculated from a knowledge of the impulsive contributions ($\delta\sigma_{33}$) to the stress (σ_{33}) at points in space and time where the temperature is varying:

$$\delta\sigma_{33}=-\gamma C\frac{\partial T}{\partial t}\delta t=-\gamma C\delta T\ , \tag{1}$$

where C is the specific heat per unit volume and γ ($=3\beta B/C$, β the thermal expansion and B the bulk modulus) is the Grüneisen parameter. The stress field is then obtained by summing over $\delta\sigma_{33}$, taking into account the phase inversion of the stress on reflection at the free surface. The expressions derived by Thomsen *et al.*[10] for the strain can be generalized for a finite optical pulse duration as follows:

$$\eta_{33}(z,t)=-\frac{\gamma C}{2\rho v^2}\times\int_{-\infty}^{\infty}\mathrm{sgn}[z-v(t-t')]\frac{\partial T}{\partial t}\bigg|_{(|z-v(t-t')|,t')}dt'\ , \tag{2}$$

where ρ is the density and the point $t'=0$ is excluded from the integral. A dimensionless parameter $D/v\zeta$

(≈ 2.5 for Au and 3.8 for Ag,[17] where D is the thermal diffusivity) determines the strain pulse shapes, shown in Fig. 3(b). The calculated displacement variations are shown by curves *b* of Figs. 1 and 2. The pulses are broadened by a factor of about 5 compared to curves *a*. However, the experimental pulse widths are still significantly (~ 2 times) broader, and the predicted asymmetric pulse shapes are not observed.

To proceed further it is necessary to consider the microscopic origin of the stress in metals. In general, the stress is related to changes in the instantaneous electron and phonon distribution functions $n_e(\mathbf{k})$ and $n_i(\mathbf{k})$ induced by the laser pulse:[10]

$$\delta\sigma_{33} = -\sum_{\mathbf{k}} \gamma_e E_{\mathbf{k}} \delta n_e(\mathbf{k}) - \sum_{\mathbf{k}} \gamma_i \hbar\omega_{\mathbf{k}} \delta n_i(\mathbf{k}) , \quad (3)$$

where $E_{\mathbf{k}}$ and $\hbar\omega_{\mathbf{k}}$ are the electron and phonon energies and $\gamma_e = -(\partial E_{\mathbf{k}}/\partial\eta_{33})/E_{\mathbf{k}}$ and $\gamma_i = -(\partial\omega_{\mathbf{k}}/\partial\eta_{33})/\omega_{\mathbf{k}}$ are the corresponding Grüneisen parameters (related to the electron and lattice deformation potentials). Solution in the general case requires a knowledge of the temporal and spatial evolution of $n_e(\mathbf{k})$ and $n_i(\mathbf{k})$, but simplification of Eq. (3) is possible if it is assumed that electron-electron and phonon-phonon couplings maintain the electron and phonon distributions in separate pseudoequilibrium states (Fermi-Dirac and Bose-Einstein distributions, respectively):

$$\delta\sigma_{33} = -\gamma_e C_e \delta T_e - \gamma_i C_i \delta T_i , \quad (4)$$

where C_e, γ_e and C_i, γ_i here refer to the specific-heat capacities (per unit volume) and average Grüneisen parameters for the electron and phonon subsystems. In Eq. (4), T_e corresponds to the temperature of the diffusing hot electron gas and T_i to that of the lattice.

The dynamics of such a system is described by two coupled nonlinear differential equations[1-7,18]

$$C_e(T_e)\frac{\partial T_e}{\partial t} = \nabla\cdot(\kappa\nabla T_e) - g(T_e - T_i) + P(z,t) , \quad (5)$$

$$C_i\frac{\partial T_i}{\partial t} = g(T_e - T_i) , \quad (6)$$

where g is the e-p coupling constant, κ the thermal conductivity,[17] and $P(z,t)$ the absorbed laser power density.[19] These equations reduce to the case of Fourier heat flow when the electrons are in thermal equilibrium with the phonons ($T_e = T_i$).[20] No diffusion term appears in Eq. (6) because the heat is almost exclusively carried by the electrons [which have a large thermal diffusivity $D_e = \kappa/C_e$, when uncoupled with the phonons, compared to the case of Fourier transport $\kappa/(C_e + C_i)$]. Solutions were obtained for $T_e(z,t)$ and $T_i(z,t)$ with a finite difference scheme,[6,21] using a Gaussian temporal profile for the laser pulse[19] and literature values of g. The calculations were then repeated with incremental changes in g until a good match to the data was obtained. At $z = 0$ in Au, for example, T_e initially increases to ~ 550 K (at $t \approx 100$ fs), whereas the maximum increase in T_i is ~ 1.3 K (at $t \approx 5$ ps). The strain pulses can be calculated from Eq. (2) by use of Eq. (4) in place of Eq. (1). However, since $\gamma_e C_e/\gamma_i C_i \lesssim 0.01$ at temperatures of a few hundred K ($C_i \approx C = 2.5\times 10^6$ Jm^{-3}K^{-1}, $C_e = AT_e = 67.6T_e$ J m^{-3}K^{-1}, $\gamma_e = 1.6$, and $\gamma_i \approx \gamma = 3.0$ for Au,[17,22] for example), the electronic contribution to the echoes associated with T_e can be neglected on picosecond time scales.[23] The strain pulses shown in Fig. 3(c) and the displacement variations shown by the curves *c* of Figs. 1 and 2 were obtained numerically from Eq. (2) (assuming $T = T_i$) using the best-fit values $g = 16(\pm 6)\times 10^{15}$ W m^{-3}K^{-1} for Au and $35(\pm 20)\times 10^{15}$ W m^{-3}K^{-1} for Ag. Taking into account measurement error and sample variations, these values are in the range of corresponding experimental estimates of g and of theoretical calculations[2-5,24] (for similar temperatures). The echo shapes are mimicked well by this model. The insets in Figs. 1 and 2 show curves for values of g near the estimated limits of error.[25] Pulse broadening occurs because the electrons are able to diffuse (at supersonic velocities) a significant distance (compared to ζ) before they lose their energy; a simple estimate of the pulse width τ_a can be obtained by considering the diffusion of the electrons over a distance $\sim z_e = (D_e t_e)^{1/2} \sim 100$ nm (assumed $\gg\zeta$) during the characteristic time $t_e = C_e/g$ (~ 1 ps) when uncoupled with the lattice: $\tau_a \sim 2z_e/v = (2/v)(\kappa/g)^{1/2} \sim 100$ ps for Au or Ag. The symmetry of the pulses is caused by the predominance of the effect of the spatial separation of the acoustic sources in Eq. (2) compared to their duration.

The fits can also be verified in the frequency domain. The surface velocity variation du_{33}/dt, or, equivalently, the time derivative of $\delta\theta$, can be shown to be directly proportional to the strain pulse shape in the one-dimensional case.[12] The frequency spectrum of the strain pulses calculated from $d\theta/dt$ is in good agreement with the nonequilibrium model, as shown for the case of Au in Fig. 4.

A similar analysis can be applied to results for films of group-VI transition metals obtained previously by the same method.[12] Values of g derived directly from the data are ~ 3 times smaller than those derived from other experiments[5] (for Cr and W) or estimated theoretically[8] (for Mo). This discrepancy may be due to additional broadening effects from acoustic attenuation at the higher frequencies involved for these metals (g is 10–20 times larger than for Au or Ag). For materials in which g

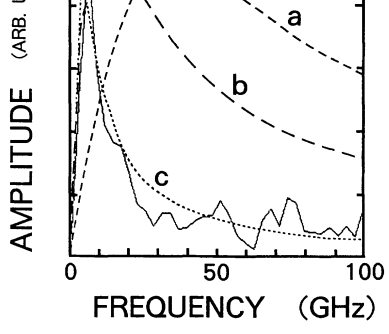

FIG. 4. Experimental phonon pulse spectrum for Au compared to the predictions of the thermoelastic model (curve *a*), the thermoelastic model including thermal diffusion (curve *b*), and the nonequilibrium model (curve *c*).

is relatively large, the use of thinner films might therefore improve the estimates of g with this method.

The success of the model of Eqs. (5) and (6) in reproducing the data for gold and silver suggests that it provides, as in other experiments, a good basis for analysis of the nonequilibrium dynamics. Recent photoemission studies[7] (for Au) and thermoreflectance measurements[3] (for Au and Ag) have shown, however, that the finite strength of the electron-electron interaction leads to a transient nonthermal hot tail in the electron-energy distribution, persisting for a time (several hundred femtoseconds) which increases with decreasing pump laser fluence. Ballistic propagation of electrons in this tail at the Fermi velocity[4,7] ($v_F = 1.4 \times 10^6$ ms^{-1} for Au), faster than electron diffusion, in principle provides an additional broadening mechanism for the strain pulse on short time scales. Initial measurements at fluences down to 0.1 mJ cm^{-2} for Au did not show any significant change in the phonon pulse shape, in accord with the predictions from Eqs. (5) and (6) for this range of fluences. Further measurements over a wider range of fluence and temperature should help to determine if the influence of these ballistic effects or other processes such as electron-imperfection scattering[4] (which impedes electron transport) can be detected.

In conclusion, the dynamics of coherent acoustic-phonon generation by femtosecond optical pulses in a metal has been investigated using gold and silver films. Striking agreement with the observed phonon pulse shapes is found by describing the nonequilibrium relaxation and diffusion of the electrons according to a model which treats the electrons and phonons as separate thermalized subsystems, thus suggesting a novel way of determining the e-p coupling constant. This constant is shown to play a central role in limiting the spectrum of acoustic frequencies generated by ultrashort light pulses in a metal.

I thank T. Hyoguchi, K. Kawashima, V. Gusev, and G. Fasol for helpful discussions.

---

*Present address: Consiglio Nazionale delle Ricerche (CNR), Istituto di Acustica "O. M. Corbino," Via Cassia 1216, I-00189 Roma, Italy.

[1]See J. G. Fujimoto, J. M. Liu, E. P. Ippen, and N. Bloembergen, Phys. Rev. Lett. **53**, 1837 (1984), and references therein.

[2]H. E. Elsayed-Ali, T. B. Norris, M. A. Pessot, and G. A. Mourou, Phys. Rev. Lett. **58**, 1212 (1987); R. W. Schoenlein, W. Z. Lin, J. G. Fujimoto, and G. L. Eesley, *ibid.* **58**, 1680 (1987); T. Juhasz, H. E. Elsayed-Ali, X. H. Hu, and W. E. Bron, Phys. Rev. B **45**, 13 819 (1992).

[3]R. H. M. Groeneveld, R. Sprik, and A. Lagendijk, Phys. Rev. B **45**, 5079 (1992).

[4]S. D. Brorson, J. G. Fujimoto, and E. P. Ippen, Phys. Rev. Lett. **59**, 1962 (1987); H. E. Elsayed-Ali, T. Juhasz, G. O. Smith, and W. E. Bron, Phys. Rev. B **43**, 4488 (1991); H. E. Elsayed-Ali and T. Juhasz, *ibid.* **47**, 13 599 (1993).

[5]S. D. Brorson, A. Kazeroonian, J. S. Moodera, D. W. Face, T. K. Cheng, E. P. Ippen, M. S. Dresselhaus, and G. Dresselhaus, Phys. Rev. Lett. **64**, 2172 (1990).

[6]G. L. Eesley, Phys. Rev. B **33**, 2144 (1986).

[7]W. S. Fann, R. Storz, H. W. K. Tom, and J. Bokor, Phys. Rev. Lett. **68**, 2834 (1992); W. S. Fann *et al.*, Phys. Rev. B **46**, 13 592 (1992).

[8]P. B. Allen, Phys. Rev. Lett. **59**, 1460 (1987); Phys. Rev. B **36**, 2920 (1987); P. B. Allen and R. C. Dynes, *ibid.* **12**, 905 (1975).

[9]P. B. Corkum, F. Brunel, N. K. Sherman, and T. Srinivasen-Rao, Phys. Rev. Lett. **61**, 2886 (1988); P. B. Corkum *et al.*, *ibid.* **64**, 1847 (1990); H. E. Elsayed-Ali, *ibid.* **64**, 1846 (1990).

[10]C. Thomsen, H. T. Grahn, H. J. Maris, and J. Tauc, Phys. Rev. B **34**, 4129 (1986).

[11]V. E. Gusev, Opt. Commun. **94**, 76 (1992).

[12]O. B. Wright and K. Kawashima, Phys. Rev. Lett. **69**, 1668 (1992); Jpn. J. Appl. Phys. **32**, 2452 (1993).

[13]O. L. Anderson, in *Physical Acoustics,* edited by W. P. Mason (Academic, New York, 1965), Vol. IIIB, p. 43.

[14]An estimate of this contribution $\delta\theta_g$ in Au and Ag is possible using the method of Ref. 12. The reflectivity $\delta R(t)$ of the films was measured, but no echoes could be resolved to an accuracy $\delta R/R \sim 10^{-6}$ at a pump fluence of 0.6 mJ cm^{-2}. Assuming photoelastic constants $dn/d\eta = d\kappa/d\eta$ [since $d\epsilon_2/d\eta \gg d\epsilon_1/d\eta$, according to Elsayed-Ali *et al.* in Ref. 4, where $\epsilon_1 + i\epsilon_2$ is the dielectric constant], $\delta\theta_g \lesssim 0.01\delta\theta$ for Au and $\lesssim 0.04\delta\theta$ for Ag.

[15]B. Lehr, H. Ulrich, and O. Weis, Z. Phys. B **48**, 23 (1982).

[16]This applies to the contribution to the strain pulse from the lattice, with a frequency spectrum centered in the 10-GHz region.

[17]*American Institute of Physics Handbook,* 3rd ed., edited by D. E. Gray (McGraw-Hill, New York, 1972).

[18]S. I. Anisimov, B. L. Kapeliovich, and T. L. Perelman, Zh. Eksp. Teor. Fiz. **66**, 776 (1974) [Sov. Phys. JETP **39**, 375 (1975)]; M. I. Kaganov, I. M. Lifshitz, and L. V. Tantarov, *ibid.* **31**, 2232 (1956) [*ibid.* **4**, 173 (1957)].

[19]I assume $P(z,t) = I_0(1-R)(1/\zeta)\exp(-z/\zeta)\exp(-t/\tau)^2$, where R is the reflectivity. The intensity I_0 is calculated from the laser fluence (equal to $\pi^{1/2}\tau I_0$).

[20]Internal consistency of the two approaches was verified by calculating the pulse shapes for a very large value of g ($> 10^{19}$ W m^{-3} K^{-1}) and recovering the Fourier conduction pulse shapes.

[21]R. Yen, Ph.D. thesis, Harvard University, 1981.

[22]T. H. K. Barron, J. G. Collins, and G. K. White, Adv. Phys. **29**, 609 (1980).

[23]For times $t \lesssim \tau_0$, the FWHM laser pulse duration, the much faster response of the electrons compared to the lattice implies a similar weighting (for the present pulse duration $\tau_0 = 200$ fs) of the two terms from Eq. (4) in Eq. (2). However, simple estimates (from Ref. 15) show that the electronic strain, in the terahertz frequency region, is completely attenuated within propagation distances $\sim 1\ \mu$m.

[24]From the theory of Allen (Ref. 8), $g = 3\hbar A\lambda\langle\omega^2\rangle/\pi k_B$, where λ is the dimensionless electron-phonon coupling parameter and $\langle\omega^2\rangle$ is the second moment of the phonon spectrum. For Au, theoretical estimates (see Ref. 5) of $\lambda\langle\omega^2\rangle$ give $g \approx 30 \times 10^{15}$ W m^{-3} K^{-1}. For Ag, approximately the same value is obtained using the results of Ref. 8 and of J. W. Lynn, H. G. Smith, and R. M. Nicklow, Phys. Rev. B **8**, 3493 (1973).

[25]Curves d and e in Fig. 1 look similar, but their FWHM widths differ by $\sim 20\%$. Deviations from the experimental curve could be judged more readily by applying a digital filter to the data of Fig. 1 with a time constant from 1 to 2 ps.